HHS Public Access

Author manuscript

Free Radic Biol Med. Author manuscript; available in PMC 2016 June 01.

Published in final edited form as:

Free Radic Biol Med. 2015 June ; 83: 227–237. doi:10.1016/j.freeradbiomed.2015.02.018.

Manganoporphyrins and Ascorbate Enhance Gemcitabine Cytotoxicity in Pancreatic Cancer

John A. Cieslak[1,2], **Robert K. Strother**[1], **Malvika Rawal**[1], **Juan Du**[1], **Claire M. Doskey**[3], **Samuel R. Schroeder**[1], **Anna Button**[4], **Brett A. Wagner**[1], **Garry R. Buettner**[1,4], and **Joseph J. Cullen**[2,4,5]

[1]Free Radical and Radiation Biology Program, Department of Radiation Oncology, University of Iowa College of Medicine, Iowa City, IA

[2]Department of Surgery, University of Iowa College of Medicine, Iowa City, IA

[3]Interdisciplinary Program in Human Toxicology, University of Iowa, Iowa City, IA

[4]Holden Comprehensive Cancer Center, Iowa City, IA

[5]Veterans Affairs Medical Center, Iowa City, IA

Abstract

Pharmacological ascorbate ($AscH^-$) selectively induces cytotoxicity in pancreatic cancer cells *vs*. normal cells *via* the generation of extracellular hydrogen peroxide (H_2O_2), producing double-stranded DNA breaks and ultimately cell death. Catalytic manganoporphyrins (MnPs) can enhance ascorbate-induced cytotoxicity by increasing the rate of $AscH^-$ oxidation and therefore the rate of generation of H_2O_2. We hypothesized that combining MnPs and $AscH^-$ with the chemotherapeutic agent gemcitabine would further enhance pancreatic cancer cell cytotoxicity without increasing toxicity in normal pancreatic cells or other organs. Redox active MnPs were combined with $AscH^-$ and administered with or without gemcitabine to human pancreatic cancer cell lines, as well as immortalized normal pancreatic ductal epithelial cells. The MnPs MnT2EPyP (Mn(III)meso-tetrakis(N-ethylpyridinium-2-yl) porphyrin pentachloride) and MnT4MPyP (Mn(III)tetrakis(N-methylpyridinium-4-yl) porphyrin pentachloride) were investigated. Clonogenic survival was significantly decreased in all pancreatic cancer cell lines studied when treated with MnP + $AscH^-$ + gemcitabine, whereas non-tumorigenic cells were resistant. The concentration of ascorbate radical ($Asc^{\bullet-}$, an indicator of oxidative flux) was significantly increased in treatment groups containing MnP and $AscH^-$. Furthermore, MnP + $AscH^-$ increased double stranded DNA breaks in gemcitabine treated cells. These results were abrogated by extracellular catalase, further supporting the role of the flux of H_2O_2. *In vivo* growth was inhibited and survival increased in mice treated with MnT2EPyP, $AscH^-$, and gemcitabine without a

Address correspondence to: Joseph J. Cullen, M.D., 1528 JCP, 200 Hawkins Drive, University of Iowa Hospitals and Clinics, Iowa City, IA 52242., joseph-cullen@uiowa.edu, W: (319) 353-8297, Fax: (319) 356-8378.

concomitant increase in systemic oxidative stress. These data suggest a promising role for the use of MnPs in combination with pharmacologic $AscH^-$ and chemotherapeutics in pancreatic cancer.

INTRODUCTION

Recent studies have demonstrated that high-dose intravenous (but not oral), pharmacological ascorbate ($AscH^-$) induces cytotoxicity and oxidative stress selectively in pancreatic cancer cells *vs*. normal cells, suggesting a promising new role as a therapeutic agent (1–4). At physiologic concentrations, ascorbate functions as a reducing agent and donor antioxidant (5). However, at pharmacological concentrations or in the presence of redox-active metal catalysts, $AscH^-$ can act as a pro-oxidant by donating an electron to oxygen, ultimately generating hydrogen peroxide (H_2O_2) (6–8). Indeed, pharmacologic ascorbate has been well established as a pro-drug for the delivery of H_2O_2 to tumors (1–3, 9, 10). Studies have also demonstrated that pharmacologic ascorbate synergizes with gemcitabine, a nucleoside analogue that has been used for advanced pancreatic cancer (11). Furthermore, recent phase I clinical trials have demonstrated pharmacologic ascorbate to be safe and well tolerated in combination with standard of care chemotherapeutics (gemcitabine + erlotinib and gemcitabine alone) for the treatment of pancreatic cancer (12, 13).

It has been proposed that that the selectivity of $AscH^-$-induced cytotoxicity toward cancer cells is a result of three major factors. First, due to a variety of factors, including increased neovascular permeability and a localized lower pH surrounding tumors, there is an increased concentration of redox active labile metal ions that can act as catalysts for the oxidation of $AscH^-$ in the extracellular space (1, 14–18); this lower pH also increases the catalytic efficiency of these metal ions (19). Second, low levels of antioxidant enzymes and high levels of endogenous ROS in cancer cells may make them more susceptible to H_2O_2-induced oxidative damage (10, 20–22). Third, erythrocytes act as a sink for ascorbate radical ($Asc^{\bullet-}$) (23) and H_2O_2 (24–26) due to redundant catabolic pathways relative to the extracellular fluid, thereby preventing accumulation of H_2O_2 in the blood and delivery to healthy tissues, while ensuring H_2O_2 delivery to the extracellular milieu.

Manganoporphyrins (MnPs) are being developed as superoxide dismutase (SOD) mimetics; however, some MnPs can also increase the flux of $AscH^-$-generated H_2O_2 *in vitro* (27–29). Recently, our laboratory has also demonstrated that MnPs can increase the rate of $AscH^-$ oxidation and steady-state levels of $Asc^{\bullet-}$ independent of their SOD-like mechanism *in vitro*, *in vivo*, and *ex vivo*. We have demonstrated that MnPs synergistically enhance $AscH^-$-induced cytotoxicity in pancreatic cancer both *in vitro* and *in vivo* (30). Furthermore, at doses relevant to clinical use in humans, these compounds have not revealed any indication of manganese toxicity or specific target organ toxicity, including those classically associated with heme porphyrins in the kidneys, liver, CNS, and heart (31).

Given that ascorbate can synergize with both gemcitabine and MnPs independently, we hypothesized that a triple therapy combining $AscH^-$, MnPs, and gemcitabine would further enhance pancreatic cancer cell cytotoxicity without increasing toxicity in normal pancreatic cells or other systemic tissues. In contrast to our previously published data, this study investigates the biological effects of combining MnPs and $AscH^-$ treatment with the

standard of care chemotherapeutic agent gemcitabine in human pancreatic cancer cell lines, and highlights the treatment's selectivity for cancer and the relative resistance of immortalized normal pancreatic ductal epithelial cells. We extend our experiments *in vivo* to mouse pancreatic cancer xenografts and additionally look for evidence of systemic oxidative stress as a result of these treatments, which has previously not been done.

MATERIALS AND METHODS

Cell Culture

The human pancreatic cancer cell lines MIA PaCa-2, Panc-1, and AsPC-1 were purchased from the American Type Culture Collection (Manassas, VA, USA) and passaged for fewer than 6 months after receipt. Cells were maintained as previously described (32). H6c7 is an immortalized cell line derived from normal pancreatic ductal epithelium with near normal genotype and phenotype of pancreatic duct epithelial cells (33) and were maintained in keratinocyte serum-free medium that was supplemented with epidermal growth factor and bovine pituitary extract. The H6c7 cells were characterized by IDEXX-RADIL (Columbia, MO, USA).

Reagents

Mn(III)tetrakis(N-methylpyridinium-4-yl) porphyrin pentachloride (MnT4MPyP), was purchased from Axxora LLC (Farmingdale, NY). Mn(III)meso-tetrakis(N-ethylpyridinium-2-yl) porphyrin pentachloride (MnT2EPyP) was from Dr. James D. Crapo (National Jewish Medical and Research Center, Denver, CO). The solids were stored at −20 °C, or in solution at 4 °C in colored vials to minimize photooxidation (34). A stock solution of 1.0 M ascorbate (pH 7.0) was made under argon and stored in screw top sealed test-tubes at 4 °C. Ascorbate concentration was verified using, ε_{265} = 14,500 M^{-1} cm^{-1} (35). The solution can be kept for several weeks without significant oxidation due to the lack of oxygen (35). A 1 mM gemcitabine (Gem) stock solution was prepared in Nanopure™ water and stored at 4 °C. Dilutions were prepared as needed.

Clonogenic Survival Assays

Clonogenic survival assays were performed as previously described (3). Briefly, for all cell types, treatments were performed for 1 h in DMEM + 10% FBS at 37 °C and 21% O_2, 48 h after initial seeding. The dishes were maintained in a 37 °C, 21% O_2, 5% CO_2 incubator for 10–14 days to allow colony formation. The colonies were then fixed with 70% ethanol, stained with Coomassie blue (10% acetic acid, 50% methanol, and 0.1% Coomassie Blue G-250), and counted (colonies containing >50 cells were scored).

Oxygen Consumption Assay

The rate of oxygen consumption (OCR, $-d[O_2]/dt$) was determined using a Clark electrode oxygen monitor (YSI Inc.) connected to an ESA Biostat multielectrode system (ESA Products, Dionex Corp.) in Dulbecco's Modified Eagle's Medium (DMEM) + 10% FBS. The effect of MnT2EPyP and MnT4MPyP on the OCR of Gem + $AscH^-$ was then determined. Accumulation of H_2O_2 was demonstrated by the addition of catalase (Sigma) to the system, with subsequent oxygen return being a direct result of the action of catalase on

the H_2O_2 that accumulated in the medium during the experiment. OCR represents the rate of production of H_2O_2; these data were combined with volume of media and number of cells to determine the flux of H_2O_2, mol cell^{-1} s^{-1}.

γH2AX Immunofluorescence

MIA PaCa-2 cells were seeded onto eight-well (0.8 cm^2/well) glass Lab-Tek Chamber slides at a density of 30,000 cells/well. After 48 h, cells were exposed to various combinations of $AscH^-$, MnPs, and Gem. When specified, cells were pretreated with catalase (50 U/mL) before the addition of the above reagents. Forty-five minutes after treatment, cells were fixed in 3% paraformaldehyde and rinsed in Dulbecco's PBS (pH 7.4). Cells were then incubated in RNAse (0.5 μg/mL) at 37 °C for 30 min; 10% normal goat serum was applied overnight for blocking of non-specific protein. Cells were incubated in anti-phospho-histone γH2AX primary antibody (1:200, Millipore) for 1.5 h. A goat anti-mouse secondary antibody conjugated to Alexa Fluor® 488 (1:500) was used as a fluorescent tag. Slides were mounted in Vectashield® with DAPI to stain the nuclei. Slides were then imaged on a Bio-Rad Radiance 2100 combination confocal and multi-photon microscope with laser sharp software. Z-plane images of each treatment were captured. The intensity of fluorescence was quantified on ImageJ ® using a maximum intensity Z-projection with identical threshold values to calculate the mean fluorescence intensity for individual cells. The mean intensity of each cell was then normalized to the area of the cell and an average intensity/area was determined. A two-tailed t-test was then performed to assign statistical significance.

In vivo Studies

All protocols were reviewed and approved by the Animal Care and Use Committee of The University of Iowa. MIA PaCa-2 tumor cells (2×10^6) were delivered subcutaneously into the hind legs of 30-day old athymic nude mice and allowed to grow until they reached between 3–5 mm in greatest dimension (10 days after injection). At that time mice were divided into 6 treatment groups, with 8 to 12 mice in each group. Treatment was then initiated and mice were treated daily for 21 days. The groups included "controls" (12 mice) that received NaCl (1 M) intraperitoneally (i.p.), daily; "gemcitabine only" (8 mice) that received gemcitabine (60 mg/kg i.p.) every 4 days; "Low MnP + Asc" (8 mice) - ascorbate (4 g/kg/d i.p.) + MnT2EPyP (0.2 mg/kg/d subcutaneously (s.c.)); "High MnP + Asc" (8 mice) - ascorbate (4 g/kg/d i.p.) + MnT2EPyP (2.0 mg/kg/d s.c.); "Low MnP Triple Therapy" (8 mice) - ascorbate (4 g/kg/d i.p.) + MnT2EPyP (0.2 mg/kg/d s.c.) + gemcitabine (60 mg/kg q 4d i.p.); and "High MnP Triple Therapy" (8 mice) - ascorbate (4 g/kg/d i.p.) + MnT2EPyP (2.0 mg/kg/d s.c.) + gemcitabine (60 mg/kg q 4d i.p.). During and after treatment, tumor size was measured every 6 to 7 days as previously described (36). Animals were sacrificed by CO_2 asphyxiation when the tumors reached 1,000 mm^3. Survival is defined as the total number of days from the first day of treatment until the time of sacrifice when the tumor volume endpoint (1,000 mm^3) was reached.

Electron paramagnetic resonance (EPR) spectra were obtained with a Bruker EMX ESR spectrometer (Bruker BioSpin), using an ER 4119HS cavity for the detection of $Asc^{\bullet-}$. EPR instrumentation settings were optimized for the detection of $Asc^{\bullet-}$: center field, 3507.62 G; sweep width, 10.00 G; receiver gain, 5.02×10^4; modulation amplitude, 0.70 G; microwave

frequency, 9.85 GHz; and nominal microwave power, 10.0 mW. To determine [$Asc^{\bullet-}$], 3-carboxy-PROXYL (3-CxP; CAS No. 2154-68-9; Sigma-Aldrich) radical was used as a standard, taking into account saturation effects (37). In separate mice that were treated for 5 days (3 mice in each treatment group), blood was drawn from the still-beating heart after a fatal dose of ketamine 1 hour after the last intraperitoneal dose of Asc, and used to: obtain EPR spectra; complete blood counts; and total glutathione (tGSH = GSH + 2GSSG), using the plate-reader based assay described in (38).

To determine systemic oxidative stress to normal organs, 4-hydroxy-2-nonenal-(4HNE)–modified protein were measured using the method described in (39). 20 mg of mouse heart, liver and kidney were washed and homogenized in 300 μL 500 mmol/L potassium phosphate, 50 mmol/L EDTA buffer pH 7.0 with Complete Mini-protease inhibitor (Roche Diagnostics). Protein (25 μg) was placed in an equal volume with Nanopure™ H_2O and blotted onto pre-wetted polyvinylidene difluoride (PVDF) membranes (Bio-Rad) and using a vacuum manifold and allowed to dry. After rewetting in methanol, the membrane was incubated in 250 mM sodium borohydride in 100 mM MOPS, pH 8.0 for 15 min to chemically reduce the Schiff base adduct to reveal the Michael addition product for antibody recognition. The membrane was then washed 3 times each with Nanopure™ H_2O followed by PBS and blocked for 30 min in 5% milk in PBS + Tween 20. The blot was incubated with the primary antibody recognizing the Michael addition product of 4HNE-modified cellular proteins (40) diluted 1/2,000 overnight at 4 °C, followed by 1.5 h in secondary antibody, horseradish peroxidase-conjugated goat anti-rabbit polyclonal antibody (1/25,000), and chemiluminescence detection (ECL Plus Western Blotting Detection System, GE Healthcare) with X-ray film. Immunoreactive protein on the dot blot was analyzed using integrated densities determined using ImageJ software.

RESULTS

MnP-Catalyzed Ascorbate Oxidation Enhances Gemcitabine-Induced Pancreatic Cancer Cytotoxicity in vitro

We hypothesized that the addition of MnPs and $AscH^-$ to gemcitabine would further increase pancreatic cancer cell cytotoxicity, either synergistically or in an additive manner. To examine this, we combined two MnPs (0.25 μM MnT2EPyP or MnT4MPyP - structures in Fig. S1) with 0.25 mM $AscH^-$. At these concentrations, the individual compounds do not effect clonogenic survival in any pancreatic cell lines, but when combined they decreased clonogenic survival in a synergistic manner (30). In the pancreatic cancer cell line MIA PaCa-2, MnT4MPyP + $AscH^-$ significantly enhanced gemcitabine toxicity, decreasing clonogenic survival at both 50 and 500 nM gemcitabine from 39.7 ± 5.0% and 35.9 ± 1.3%, to 6.7 ± 0.9% and 1.0 ± 0.4%, respectively, *vs*. the equivalent doses of gemcitabine alone (*, $P < 0.01$, Fig 1A). Furthermore, the addition of MnT4MPyP + $AscH^-$ to gemcitabine significantly decreased clonogenic survival at both 50 and 500 nM gemcitabine *vs*. MnT4MPyP + $AscH^-$ alone (*, $P < 0.01$). As previously shown, combination of MnT4MPyP + $AscH^-$ without added chemotherapy can also significantly decreasing clonogenic survival *vs*. controls (#, $P < 0.01$).

Next, we investigated the affect of adding MnT2EPyP + $AscH^-$ to gemcitabine on clonogenic survival, again in MIA PaCa-2 cells. MnT2EPyP + $AscH^-$ appeared to have greater cytotoxicity when combined with gemcitabine compared to MnT4MPyP + $AscH^-$ + gemcitabine, completely eliminating clonogens at both 50 and 500 nM gemcitabine (*, $P < 0.01$, Fig. 1B). Again, the addition of MnT2EPyP + $AscH^-$ to gemcitabine significantly decreased clonogenic survival at both 50 and 500 nM gemcitabine *vs*. MnT2EPyP + $AscH^-$ alone (*, $P < 0.01$). To establish a dose response, the experiment was repeated using MnT2EPyP (0.1 μM) + $AscH^-$ (1 mM). Under these conditions, the normalized clonogenic survival was significantly reduced, but not eliminated at both 50 and 500 nM gemcitabine, from 23.3 ± 1.8% and 19.0 ± 0.3%, to 1.3 ± 0.9% and 0.4 ± 0.2%, respectively, *vs*. the equivalent doses of gemcitabine alone (*, $P < 0.01$, Fig. 1B). Even at the lower dose, MnT2EPyP + $AscH^-$ and gemcitabine significantly decreased clonogenic survival at both 50 and 500 nM gemcitabine *vs*. MnT2EPyP + $AscH^-$ alone (*, $P < 0.01$). In both sets of concentrations combination MnT2EPyP + $AscH^-$ without chemotherapy also statistically reduced clonogenic survival *vs.* controls (#, $P < 0.01$).

To determine if the increase in cytotoxicity upon the addition of MnPs + $AscH^-$ to gemcitabine can be explained by a resulting increase in the production of H_2O_2, oxygen consumption rate (OCR) was determined (Fig. S1). OCR measured in DMEM (10% FBS) was significantly increased upon the addition of MnPs to $AscH^-$ (≈2-fold increase for both MnT4MPyP and MnT2EPyP). The addition of gemcitabine before (Fig. S1A), or after (Fig. S1B) MnP + $AscH^-$ had no effect on OCR, suggesting a cytotoxic mechanism independent of H_2O_2 flux.

We then extended our findings in MIA PaCa-2 cells to two additional pancreatic cancer cell lines, PANC-1 and AsPC-1. Again, the addition of MnPs + $AscH^-$ to gemcitabine significantly reduced the clonogenic survival compared to gemcitabine alone (*, $P < 0.01$ using MnT4MPyP + $AscH^-$ in PANC-1, Fig. 1C, and *, $P < 0.01$ using MnT2EPyP + $AscH^-$ in ASPC-1, Fig. 1D). Of note, whereas the addition of MnT2EPyP + $AscH^-$ to gemcitabine significantly decreased clonogenic survival at both 50 and 500 nM gemcitabine *vs*. MnT2EPyP + $AscH^-$ alone in AsPC-1 cells (*, $P < 0.01$), the addition of MnT4MPyP + $AscH^-$ to gemcitabine did not significantly decrease clonogenic survival when compared to MnT4MPyP + $AscH^-$ without gemcitabine in PANC-1 cells. In both AsPC-1 and PANC-1 cell lines, the combination of MnP + $AscH^-$ without gemcitabine was enough to statistically decrease clonogenic survival *vs.* controls (#, $P < 0.01$).

Catalase Rescues MnP + $AscH^-$ + Gemcitabine - Induced Cytotoxicity

Pharmacologic ascorbate has been well established as a pro-drug for the delivery of peroxide to tumors (1–3, 10) and MnPs can act as catalysts to increase the rate of H_2O_2 production (30). To determine if H_2O_2 flux mediates MnP + $AscH^-$ cytotoxicity when combined with gemcitabine *in vitro*, we pretreated cells with extracellular catalase which reversed the decrease in clonogenic survival observed (*, $P < 0.01$, Fig. 1E). These data support H_2O_2 as the mediator of the enhanced pancreatic cell cytotoxicity induced by MnP + $AscH^-$.

Non-tumorigenic Cells Are Resistant to MnP + AscH⁻-Enhanced Gemcitabine Cytotoxicity in vitro

To investigate whether MnP + AscH⁻ and gemcitabine would also selectively cause pancreatic cancer cell death, we repeated clonogenic survival assays on MIA PaCa-2 and H6c7 cells. H6c7 is an immortalized cell line derived from normal pancreatic ductal epithelium with near normal genotype and phenotype of pancreatic duct epithelial cells (33). Cells were treated with 50 and 500 nM gemcitabine, 0.25 μM MnP (MnT4MPyP or MnT2EPyP) + 0.25 mM AscH⁻, or a combination of MnP (0.25 μM) + AscH⁻ (0.25 mM) + gemcitabine (50 and 500 nM). In both the control group and gemcitabine (50 nM) group, there was no significant difference in plating efficiency between MIA PaCa-2 and H6c7 cells. However, when cells were treated with MnT4MPyP (0.25 μM) + AscH⁻ (0.25 mM) with or without gemcitabine (50 and 500 nM), there was significantly more cytotoxicity in MIA PaCa-2 cells *vs*. H6c7 cells, *i.e*. normal cells were much more resistant to treatment (*, $P < 0.01$, Fig. 2A). The same sensitivity was observed in cells treated with MnT2EPyP (*, $P < 0.01$, Fig. 2B). Interestingly, when cells were treated with 500 nM gemcitabine alone, H6c7 cells were significantly more sensitive to treatment than MIA PaCa-2 cells at that dose (*, $P < 0.01$, Fig. 2A,B).

MnP + AscH⁻ and Gemcitabine Increase DNA Damage

Ascorbate-induced cell death occurs *via* H_2O_2-mediated DNA damage and increased oxidative stress (3). It is hypothesized that this increase in DNA damage and reactive oxygen species triggers autophagy, a fusion of autophagosomes and lysosomes resulting in the formation of consumptive autophagolysosomes, followed by caspase-independent cell death (41, 42). Gemcitabine acts as a nucleoside analogue and chain terminator. It mediates its potent anti-tumor effect *via* p53 and PUMA in a transcription-dependent manner (43). We hypothesized that a combination of MnP + AscH⁻ + gemcitabine, would induce DNA damage in tumor cells to a greater degree than either treatment alone. To visualize and quantitate DNA damage we performed immunohistochemistry for γH2AX. It has been well established as a marker for double-stranded DNA breaks (44).

MnP + AscH⁻ and MnP + AscH⁻ + gemcitabine-treated MIA PaCa-2 cells had significantly more γH2AX fluorescence present than cells treated with gemcitabine, MnP or Asc alone. Overall, there was an increase in green fluorescent puncta observed in cells treated with MnT4MPyP + AscH⁻ or MnT4MPyP + AscH⁻ + gemcitabine (Fig. 3A), and MnT2EPyP + AscH⁻ or MnT2EPyP + AscH⁻ + gemcitabine (Fig. 3C), indicating an increase in the amount of double stranded DNA breaks present. Indeed, when the fluorescence per area was quantified, MnT4MPyP + AscH⁻ and MnT4MPyP + AscH⁻ + gemcitabine showed significant increases in γH2AX fluorescence compared to control, gemcitabine, MnT4MPyP, and AscH⁻ treated cells ($P < 0.01$, Fig. 3B), though no difference between MnT4MPyP + AscH⁻ and MnT4MPyP + AscH⁻ + gemcitabine was observed. There was also a clear visual increase in γH2AX fluorescence in cells treated with MnT2EPyP + AscH⁻ and MnT2EPyP + AscH⁻ + gemcitabine (Fig. 3C). When quantified, an increase in γH2AX fluorescence was observed in cells treated with MnT2EPyP + AscH⁻ or MnT2EPyP + AscH⁻ + gemcitabine *vs*. control, gemcitabine and MnT2EPyP-treated cells, with only MnT2EPyP + AscH⁻ treated cells showing significantly increased γH2AX fluorescence

compared to $AscH^-$ alone ($P < 0.05$, Fig. 3D). Again, there was no difference observed as the result of the addition of MnT2EPyP + $AscH^-$ to gemcitabine.

Taken collectively, these data indicate that MnPs + $AscH^-$ increase the amount of DNA damage observed when combined with gemcitabine, *vs*. gemcitabine therapy alone. However, while MnT2EPyP + $AscH^-$ + gemcitabine does significantly decrease clonogenic survival *vs*. MnT2EPyP + $AscH^-$ (Fig. 1), there is no difference in double stranded DNA breaks observed between MnT2EPyP + $AscH^-$ and MnT2EPyP + $AscH^-$ + gemcitabine. This observation can likely be explained by gemcitabine's mechanism of transcriptional chain termination *vs*. $AscH^-$-induced, H_2O_2-mediated double stranded DNA damage, which does not recruit γH2AX in the same way. This is supported by the fact that there were no differences in γH2AX fluorescence in gemcitabine-only treated cells *vs*. controls, whereas an increase in γH2AX fluorescence was observed with $AscH^-$ treatment.

To demonstrate H_2O_2 flux as the primary determinant of MnP + $AscH^-$ + gemcitabine-induced cytotoxicity, γH2AX immunohistochemistry was repeated with both MnPs in the presence and absence of catalase (Fig. 3E). When treated with catalase, the green fluorescent puncta observed in MnT4MPyP + $AscH^-$ + gemcitabine and MnT2EPyP + $AscH^-$ + gemcitabine-treated cells were absent, which was confirmed by quantification of the fluorescence ($P < 0.01$, Fig. 3F).

MnP + $AscH^-$ Enhances Gemcitabine-Induced Pancreatic Cancer Cytotoxicity in vivo

To determine if the MnP and $AscH^-$ with gemcitabine would be effective *in vivo*, we treated mice with pre-established MIA PaCa-2 human pancreatic tumor xenografts. As it was unknown if the combination of MnT2EPyP (MnP) + $AscH^-$ + gemcitabine would be toxic to the mice, we created both a high and low dose MnT2EPyP + $AscH^-$ treatment group, with and without gemcitabine. Throughout the course of the experiment there were no significant changes in weight among the 6 treatment groups, and none of the animals had to be sacrificed for weight loss or cachexia.

MnP + $AscH^-$ + gemcitabine significantly inhibited tumor growth when high dose MnP was used, as compared to mice treated with saline (controls), gemcitabine alone (*, $P < 0.01$, Fig. 4A), or the combination of "Low MnP + $AscH^-$" (#, $P < 0.01$), Fig. 4A). Mice were sacrificed once tumors reached a volume of 1000 mm^3 (a pre-determined endpoint that complies with requirements set by the Animal Care and Use Committee of The University of Iowa). Day-27 of the study was the first time point at which mice began to reach the tumor volume requiring sacrifice; analysis of tumor volume was performed at that time. On day 27, the control group had a mean tumor volume of 649 ± 88 mm^3 whereas the gemcitabine group had a mean tumor volume of 525 ± 131 mm^3. In mice treated with a combination of MnP + $AscH^-$, mean tumor volumes were 520 ± 91 mm^3 with "Low MnP + $AscH^-$," and 384 ± 94 mm^3 with "High MnP + $AscH^-$". In mice treated with MnP + $AscH^-$ + gemcitabine triple therapy, tumor growth was further inhibited with mean tumor volumes of 242 ± 40 mm^3 and 108 ± 22 mm^3, with "Low" and "High MnP," respectively (means ± SEM). While a statistically significant inhibition of tumor growth can be demonstrated on day 27 of the experiment, no conclusions can be drawn about the duration of this inhibitory effect beyond day 27. We next examined the time for mice in the different treatment groups

to reach the experimental endpoint (tumor volume of 1000 mm^3). Mice treated with "High MnP + $AscH^-$ + gemcitabine" had a significantly increased number of mice with tumors smaller than 1000 mm^3 *vs*. control mice (*, $P < 0.01$), Fig. 4B), with 71% at day 69 *vs*. 33% of control mice, 12.5% of gemcitabine only mice, 25% of "Low MnP + $AscH^-$" mice, 33% of "High MnP + $AscH^-$" mice, and 37.5% of "Low MnP + $AscH^-$ + gemcitabine" animals.

In order to determine the effect of treatment on [$Asc^{\bullet -}$], a direct correlate for the rate of $AscH^-$ oxidation and rate of H_2O_2 production (and therefore the potential for cancer cell cytotoxicity), we also obtained whole blood from separate groups of mice treated with the compounds used above. As expected, $Asc^{\bullet -}$ was below the limit of detection in whole blood drawn from mice treated with saline (Fig. 4C); when MnT2EPyP (0.2 mg/kg) was administered subcutaneously, EPR detectable $Asc^{\bullet -}$ in the blood was increased from undetectable to 34 ± 2 nmol/L. Following intraperitoneal administration of $AscH^-$ (4 g/kg), EPR detectable $Asc^{\bullet -}$ further increased to 99 ± 11 nmol/L. In mice treated with MnT2EPyP and $AscH^-$, $Asc^{\bullet -}$ in the blood significantly increased to 239 ± 17 nmol/L. Finally, in mice treated with MnT2EPyP + $AscH^-$ + gemcitabine (60 mg/kg i.p. q 4 days) triple therapy, $Asc^{\bullet -}$ in the blood was increased to 160 ± 35 nmol/L. Therefore, while MnT2EPyP + $AscH^-$ + gemcitabine significantly increased [$Asc^{\bullet -}$] *vs*. control ($P < 0.01$) and MnT2EPyP-treated mice ($P < 0.05$), there was no difference in [$Asc^{\bullet -}$] when compared to MnT2EPyP + $AscH^-$-treated mice. These data are consistent with γH2AX immunohistochemistry findings *in vitro* (Fig. 3). As [$Asc^{\bullet -}$] increases, H_2O_2 flux increases, leading to increased double stranded DNA breaks from increased oxidative stress, as seen with the γH2AX fluorescence.

Combination MnP + $AscH^-$ and Gemcitabine Does Not Alter Systemic Oxidative Stress

To assess systemic oxidative stress *in vivo*, immunoreactive 4-hydroxy-2-nonenal-(4HNE) modified protein levels were analyzed in the hearts, livers and kidneys of mice treated with MnT2EPyP, $AscH^-$, MnT2EPyP + $AscH^-$, or MnT2EPyP + $AscH^-$ + gemcitabine. A representative dot blot analysis of heart homogenates harvested from mice treated for 5 consecutive days (as described above), is shown in Fig. 5A. Similar dot blots were also performed for liver and kidney homogenates. Quantification of the integrated density of each blot revealed no differences in 4HNE-modified protein in the heart, liver, or kidneys of mice treated with MnT2EPyP + $AscH^-$ + gemcitabine *vs*. controls (Fig. 5B). These data support the hypothesis that a combination of MnT2EPyP + $AscH^-$ + gemcitabine can effectively increase tumor specific cytotoxicity without causing increased systemic oxidative damage *via* lipid peroxidation in normal tissues or end organs.

We hypothesize that the selectivity of $AscH^-$-induced cytotoxicity to tumor *vs.* normal tissue is in part due to the ability of erythrocytes to act as a sink for $Asc^{\bullet -}$ and H_2O_2 in the systemic circulation (23–26). Thus, due to abundant and robust catabolic pathways present in red blood cells (RBC) relative to the extracellular fluid, peroxide buildup in the blood and delivery to healthy tissues is minimized. To investigate the effect of MnP + $AscH^-$ therapy on hematologic cells, mice were treated as described above before blood was harvested for complete blood counts (CBC) and differential analysis. Examination of the CBCs did not reveal significant differences in RBC or WBC counts, leukocyte or lymphocyte percentages, or hemoglobin concentration (Fig. 6A). Indeed, the only abnormality noted was a

hemoconcentration effect observed in mice receiving $AscH^-$ alone or $AscH^-$ in combination with MnT2EPyP (hematocrit, $P < 0.05$, Fig. 6A). Though not significant, hemoglobin concentrations also trended toward increasing after a treatment that included $AscH^-$. This can be explained by the large hyperosmolar load that results from the administration of pharmacological ascorbate.

To investigate the effect of treatment on the reducing capacity of erythrocytes, the intracellular glutathione concentration was measured in RBCs harvested from mice following 5 days of treatment. Erythrocyte glutathione (GSH) represents the largest antioxidant pool in the body, and is likely responsible for the consumption of excess $Asc^{\bullet -}$ and H_2O_2 produced after the administration of $AscH^-$. Interestingly, intracellular [GSH] was significantly lower in all treatment groups *vs*. controls (*, $P < 0.01$, #, $P < 0.05$, Fig. 6B) indicating an overall global consumption of glutathione in RBCs after introduction of a pro-oxidant agent. This was most surprising in the case of MnT2EPyP, as this compound alone had little to no effect on [$Asc^{\bullet -}$] (Fig. 4C), γH2AX fluorescence (Fig. 3A,B), or clonogenic survival (data not shown) when administered alone. However, these data and the high capacity of RBCs to remove extracellular H_2O_2 ($k_{cell} = 2.9 \times 10^{-12}$ s^{-1} $cell^{-1}$ L (36)) support the hypothesis that erythrocytes may act as a systemic buffer to H_2O_2 and oxidative stress. Furthermore, when considered in combination with 4HNE-modified protein analysis (Fig. 5), these data suggest that the “erythrocyte sink” may be robust enough to prevent systemic oxidative damage from treatment with MnP + $AscH^-$ + gemcitabine triple therapy.

DISCUSSION

Pharmacologic ascorbate induces cytotoxicity selectively in pancreatic cancer cells *in vitro* and *in vivo* and has been determined as safe and well-tolerated in clinical trials (1, 2, 10, 13, 41, 45). Millimolar plasma concentrations of $AscH^-$ and the presence of catalytic metal ions are keys for promoting the pro-oxidative effects of $AscH^-$ in the extracellular fluid, where ascorbate acts as a pro-drug for the generation of H_2O_2. High levels of $AscH^-$ can also increase the level of labile iron in tumors (46). Increased oxidation of $AscH^-$ results in a higher flux of H_2O_2, ultimately resulting in greater tumor toxicity. Alternatively, hindering the removal of H_2O_2 by the peroxide-removal system can also increase tumor cytotoxicity (47). Therefore, agents that either enhance the oxidation rate of $AscH^-$ or inhibit the removal of H_2O_2 (thereby increasing steady-state levels of H_2O_2 in tumor tissue) are desirable for increased efficacy in ascorbate-based therapeutic strategies.

Manganoporphyrins are redox active catalysts, have been studied extensively *in vitro* and *in vivo*, and are well suited for this purpose (27, 48–50). Gemcitabine, adjuvant chemotherapy for advanced pancreatic cancer, has previously been shown to act synergistically with pharmacological ascorbate (11). Because MnPs and gemcitabine each individually synergize with pharmacologic ascorbate, we reasoned that a triple therapy combination of MnP + $AscH^-$ + gemcitabine would further enhance pancreatic cancer cytotoxicity. Indeed, we have demonstrated that MnPs and ascorbate work synergistically with gemcitabine to enhance cytotoxicity *vs.* MnP + $AscH^-$ alone in pancreatic cancer *in vitro*, and *in vivo*. The cytotoxic mechanism of action of ascorbate promoting H_2O_2 flux and double-stranded DNA breaks was demonstrated using catalase rescue of clonogenic plating efficiency and γH2AX

immunohistochemistry. However, the synergism of MnP + $AscH^-$ + gemcitabine does not seem to result from an increase in the oxidation rate of $AscH^-$ alone, as the OCR and [$Asc^{\bullet -}$] resulting from the addition of gemcitabine was not significantly different from MnP + $AscH^-$ without gemcitabine. Intuitively, this is not unexpected, as gemcitabine is a known nucleoside analogue and does not affect the rate of $AscH^-$ oxidation or H_2O_2 production itself. We therefore propose that the enhanced cytotoxicity observed with MnP + $AscH^-$ + gemcitabine triple therapy is the result of two independent biological insults imparted upon tumor cells: increased oxidative damage from H_2O_2 and reactive oxygen species as a result of MnP-promoted $AscH^-$ oxidation and the inhibition of DNA synthesis and cancer proliferation as a result of the chain terminating effects of gemcitabine.

Our laboratory has previously demonstrated that MnPs enhance $AscH^-$-induced cytotoxicity in pancreatic cancer both *in vitro* and *in vivo* in a synergistic manner (30). We concluded that the combination of MnPs and $AscH^-$ may be effective as a cancer therapy. In this new study, we present an extension of those results by demonstrating the potential efficacy of a clinically relevant chemotherapeutic regimen by combining MnPs, $AscH^-$ and gemcitabine to achieve enhanced cytotoxicity in pancreatic cancer *in vitro*, and *in vivo*. (28–30). Of note, in our previously published paper (30), the MnP + $AscH^-$ treatment was more effective at inhibiting tumor growth than observed in the current study (Fig. 4A). This may be explained by the fact that in our current experiment, mice were treated with MnT2EPyP and in our previous study the mice were treated with MnT4MPyP. The MnT4MPyP compound generates H_2O_2 at a faster rate (the slope of O_2 consumption is much steeper *in vitro* (Fig. S1)). Therefore, this may translate into a greater effect *in vivo* as MnT4MPyP produces a greater flux of H_2O_2 per cell which is the determining factor in MnP + $AscH^-$ induced cytotoxicity.

In the current study, we have demonstrated the selectivity of MnP + $AscH^-$ + gemcitabine therapy to cancer cells by demonstrating the resistance of normal tissues using immortalized pancreatic ductal epithelial cells in clonogenic survival assays, as well as the absence of increased systemic oxidative stress *in vivo* using 4HNE modified protein analysis. Additionally, there was no revealed immunosuppression or anemia in treatment groups, though erythrocyte levels of glutathione were decreased in all treatments compared to control mice. Collectively, these data suggest that while an overall increase in tumor oxidative stress may result from treatment, the ability of the blood to remove excess H_2O_2 and buffer the oxidative insult prevents damage to normal tissues.

Whereas these results are promising, it must be remembered that the use of mouse xenografts for *in vivo* analysis of antitumor therapy is an imperfect model. For one, tumor microenvironment and stromal elements play an essential role in in tumor genetic and epigenetic changes, metastatic transformation, and response to therapy in pancreatic cancer (51). Certainly, the tumor environment of a pancreatic tumor xenograft in the mouse hind limb does not fully reflect tumor behavior in the pancreas. This can be addressed through the development of orthotopic models for pancreatic cancer, though these are not without their own difficulties - including cost, specialized skill required for tumor engraftment, and tumor growth monitoring. Therefore, though the data presented in this paper are encouraging,

further studies are necessary to determine the efficacy of MnP, $AscH^-$, and gemcitabine therapy and ultimately human trials will be required.

In summary, combination MnP, $AscH^-$, and gemcitabine may provide an enhanced cytotoxic therapy for the treatment of pancreatic cancer and occurs without causing an increase in systemic oxidative stress. Furthermore, MnPs, and $AscH^-$ + gemcitabine have independently been deemed safe in clinical trials. Therefore, we conclude that there is a promising role for the use of MnPs in combination with pharmacologic $AscH^-$ and standard of care chemotherapeutics in the treatment of pancreatic cancer, and phase I clinical trials of this triple therapy are justified.

Supplementary Material

Refer to Web version on PubMed Central for supplementary material.

Acknowledgments

Supported by NIH grants CA166800, CA078586, R01CA169046, the Susan L. Bader Foundation of Hope, and a Merit Review grant from the Medical Research Service, Department of Veterans Affairs 1I01BX001318-01A2.

References

1. Chen Q, Espey MG, Krishna MC, Mitchell JB, Corpe CP, Buettner GR, et al. Pharmacologic ascorbic acid concentrations selectively kill cancer cells: action as a pro-drug to deliver hydrogen peroxide to tissues. Proceedings of the National Academy of Sciences of the United States of America. 2005 Sep 20; 102(38):13604–9. [PubMed: 16157892]
2. Chen Q, Espey MG, Sun AY, Lee JH, Krishna MC, Shacter E, et al. Ascorbate in pharmacologic concentrations selectively generates ascorbate radical and hydrogen peroxide in extracellular fluid in vivo. Proceedings of the National Academy of Sciences of the United States of America. 2007 May 22; 104(21):8749–54. [PubMed: 17502596]
3. Du J, Martin SM, Levine M, Wagner BA, Buettner GR, Wang SH, et al. Mechanisms of ascorbate-induced cytotoxicity in pancreatic cancer. Clinical cancer research: an official journal of the American Association for Cancer Research. 2010 Jan 15; 16(2):509–20. [PubMed: 20068072]
4. Levine M, Padayatty SJ, Espey MG. Vitamin C: a concentration-function approach yields pharmacology and therapeutic discoveries. Advances in nutrition. 2011 Mar; 2(2):78–88. [PubMed: 22332036]
5. Buettner GR. The pecking order of free radicals and antioxidants: lipid peroxidation, alpha-tocopherol, and ascorbate. Archives of biochemistry and biophysics. 1993 Feb 1; 300(2):535–43. [PubMed: 8434935]
6. Buettner GR, Jurkiewicz BA. Catalytic metals, ascorbate and free radicals: combinations to avoid. Radiation research. 1996 May; 145(5):532–41. [PubMed: 8619018]
7. Frei B, Lawson S. Vitamin C and cancer revisited. Proceedings of the National Academy of Sciences of the United States of America. 2008 Aug 12; 105(32):11037–8. [PubMed: 18682554]
8. Halliwell B. Vitamin C: poison, prophylactic or panacea? Trends in biochemical sciences. 1999 Jul; 24(7):255–9. [PubMed: 10390611]
9. Chen Q, Espey MG, Sun AY, Pooput C, Kirk KL, Krishna MC, et al. Pharmacologic doses of ascorbate act as a prooxidant and decrease growth of aggressive tumor xenografts in mice. Proceedings of the National Academy of Sciences of the United States of America. 2008 Aug 12; 105(32):11105–9. [PubMed: 18678913]
10. Du J, Cullen JJ, Buettner GR. Ascorbic acid: chemistry, biology and the treatment of cancer. Biochimica et biophysica acta. 2012 Dec; 1826(2):443–57. [PubMed: 22728050]

11. Espey MG, Chen P, Chalmers B, Drisko J, Sun AY, Levine M, et al. Pharmacologic ascorbate synergizes with gemcitabine in preclinical models of pancreatic cancer. Free radical biology & medicine. 2011 Jun 1; 50(11):1610–9. [PubMed: 21402145]
12. Monti DA, Mitchell E, Bazzan AJ, Littman S, Zabrecky G, Yeo CJ, et al. Phase I evaluation of intravenous ascorbic acid in combination with gemcitabine and erlotinib in patients with metastatic pancreatic cancer. PloS one. 2012; 7(1):e29794. [PubMed: 22272248]
13. Welsh JL, Wagner BA, van't Erve TJ, Zehr PS, Berg DJ, Halfdanarson TR, et al. Pharmacological ascorbate with gemcitabine for the control of metastatic and node-positive pancreatic cancer (PACMAN): results from a phase I clinical trial. Cancer chemotherapy and pharmacology. 2013 Mar; 71(3):765–75. [PubMed: 23381814]
14. Baronzio G, Schwartz L, Kiselevsky M, Guais A, Sanders E, Milanesi G, et al. Tumor interstitial fluid as modulator of cancer inflammation, thrombosis, immunity and angiogenesis. Anticancer research. 2012 Feb; 32(2):405–14. [PubMed: 22287726]
15. Casciari JJ, Riordan NH, Schmidt TL, Meng XL, Jackson JA, Riordan HD. Cytotoxicity of ascorbate, lipoic acid, and other antioxidants in hollow fibre in vitro tumours. British journal of cancer. 2001 Jun 1; 84(11):1544–50. [PubMed: 11384106]
16. Halliwell B. Oxygen radicals, nitric oxide and human inflammatory joint disease. Annals of the rheumatic diseases. 1995 Jun; 54(6):505–10. [PubMed: 7632097]
17. Klockars M, Weber T, Tanner P, Hellstrom PE, Pettersson T. Pleural fluid ferritin concentrations in human disease. Journal of clinical pathology. 1985 Jul; 38(7):818–24. [PubMed: 4019803]
18. Weinberger A, Simkin PA. Plasma proteins in synovial fluids of normal human joints. Seminars in arthritis and rheumatism. 1989 Aug; 19(1):66–76. [PubMed: 2672342]
19. Schafer FQ, Buettner GR. Acidic pH amplifies iron-mediated lipid peroxidation in cells. Free radical biology & medicine. 2000 Apr 15; 28(8):1175–81. [PubMed: 10889446]
20. Liu J, Hinkhouse MM, Sun W, Weydert CJ, Ritchie JM, Oberley LW, et al. Redox regulation of pancreatic cancer cell growth: role of glutathione peroxidase in the suppression of the malignant phenotype. Human gene therapy. 2004 Mar; 15(3):239–50. [PubMed: 15018733]
21. Oberley LW. Mechanism of the tumor suppressive effect of MnSOD overexpression. Biomedicine & pharmacotherapy = Biomedecine & pharmacotherapie. 2005 May; 59(4):143–8. [PubMed: 15862707]
22. Schafer FQ, Buettner GR. Redox environment of the cell as viewed through the redox state of the glutathione disulfide/glutathione couple. Free radical biology & medicine. 2001 Jun 1; 30(11): 1191–212. [PubMed: 11368918]
23. May JM, Qu Z, Cobb CE. Recycling of the ascorbate free radical by human erythrocyte membranes. Free radical biology & medicine. 2001 Jul 1; 31(1):117–24. [PubMed: 11425497]
24. Wagner BA, Witmer JR, van't Erve TJ, Buettner GR. An Assay for the Rate of Removal of Extracellular Hydrogen Peroxide by Cells. Redox biology. 2013; 1(1):210–7. [PubMed: 23936757]
25. Brown JM, Grosso MA, Terada LS, Beehler CJ, Toth KM, Whitman GJ, et al. Erythrocytes decrease myocardial hydrogen peroxide levels and reperfusion injury. The American journal of physiology. 1989 Feb; 256(2 Pt 2):H584–8. [PubMed: 2916691]
26. Low FM, Hampton MB, Winterbourn CC. Peroxiredoxin 2 and peroxide metabolism in the erythrocyte. Antioxidants & redox signaling. 2008 Sep; 10(9):1621–30. [PubMed: 18479207]
27. Batinic-Haberle I, Reboucas JS, Spasojevic I. Superoxide dismutase mimics: chemistry, pharmacology, and therapeutic potential. Antioxidants & redox signaling. 2010 Sep 15; 13(6): 877–918. [PubMed: 20095865]
28. Tian J, Peehl DM, Knox SJ. Metalloporphyrin synergizes with ascorbic acid to inhibit cancer cell growth through fenton chemistry. Cancer biotherapy & radiopharmaceuticals. 2010 Aug; 25(4): 439–48. [PubMed: 20735206]
29. Ye X, Fels D, Tovmasyan A, Aird KM, Dedeugd C, Allensworth JL, et al. Cytotoxic effects of Mn(III) N-alkylpyridylporphyrins in the presence of cellular reductant, ascorbate. Free radical research. 2011 Nov; 45(11–12):1289–306. [PubMed: 21859376]

30. Rawal M, Schroeder SR, Wagner BA, Cushing CM, Welsh JL, Button AM, et al. Manganoporphyrins increase ascorbate-induced cytotoxicity by enhancing H2O2 generation. Cancer research. 2013 Aug 15; 73(16):5232–41. [PubMed: 23764544]

31. Gad SC, Sullivan DW Jr, Crapo JD, Spainhour CB. A nonclinical safety assessment of MnTE-2-PyP, a manganese porphyrin. International journal of toxicology. 2013 Jul; 32(4):274–87. [PubMed: 23704100]

32. Teoh ML, Sun W, Smith BJ, Oberley LW, Cullen JJ. Modulation of reactive oxygen species in pancreatic cancer. Clinical cancer research: an official journal of the American Association for Cancer Research. 2007 Dec 15; 13(24):7441–50. [PubMed: 18094428]

33. Qian J, Niu J, Li M, Chiao PJ, Tsao MS. In vitro modeling of human pancreatic duct epithelial cell transformation defines gene expression changes induced by K-ras oncogenic activation in pancreatic carcinogenesis. Cancer research. 2005 Jun 15; 65(12):5045–53. [PubMed: 15958547]

34. Maliyackel AC, Otvos JW, Spreer LO, Calvin M. Photoinduced oxidation of a water-soluble manganese(III) porphyrin. Proceedings of the National Academy of Sciences of the United States of America. 1986 Jun; 83(11):3572–4. [PubMed: 16593699]

35. Buettner GR. In the absence of catalytic metals ascorbate does not autoxidize at pH 7: ascorbate as a test for catalytic metals. Journal of biochemical and biophysical methods. 1988 May; 16(1):27–40. [PubMed: 3135299]

36. Euhus DM, Hudd C, LaRegina MC, Johnson FE. Tumor measurement in the nude mouse. Journal of surgical oncology. 1986 Apr; 31(4):229–34. [PubMed: 3724177]

37. Buettner GR, Kiminyo KP. Optimal EPR detection of weak nitroxide spin adduct and ascorbyl free radical signals. Journal of biochemical and biophysical methods. 1992 Mar; 24(1–2):147–51. [PubMed: 1313843]

38. Rahman I, Kode A, Biswas SK. Assay for quantitative determination of glutathione and glutathione disulfide levels using enzymatic recycling method. Nature protocols. 2006; 1(6):3159–65.

39. Allen BG, Bhatia SK, Buatti JM, Brandt KE, Lindholm KE, Button AM, et al. Ketogenic diets enhance oxidative stress and radio-chemo-therapy responses in lung cancer xenografts. Clinical cancer research: an official journal of the American Association for Cancer Research. 2013 Jul 15; 19(14):3905–13. [PubMed: 23743570]

40. Cohn JA, Tsai L, Friguet B, Szweda LI. Chemical characterization of a protein-4-hydroxy-2-nonenal cross-link: immunochemical detection in mitochondria exposed to oxidative stress. Archives of biochemistry and biophysics. 1996 Apr 1; 328(1):158–64. [PubMed: 8638925]

41. Chen Y, McMillan-Ward E, Kong J, Israels SJ, Gibson SB. Oxidative stress induces autophagic cell death independent of apoptosis in transformed and cancer cells. Cell death and differentiation. 2008 Jan; 15(1):171–82. [PubMed: 17917680]

42. Ohtani S, Iwamaru A, Deng W, Ueda K, Wu G, Jayachandran G, et al. Tumor suppressor 101F6 and ascorbate synergistically and selectively inhibit non-small cell lung cancer growth by caspase-independent apoptosis and autophagy. Cancer research. 2007 Jul 1; 67(13):6293–303. [PubMed: 17616688]

43. Hill R, Rabb M, Madureira PA, Clements D, Gujar SA, Waisman DM, et al. Gemcitabine-mediated tumour regression and p53-dependent gene expression: implications for colon and pancreatic cancer therapy. Cell death & disease. 2013; 4:e791. [PubMed: 24008735]

44. Sharma A, Singh K, Almasan A. Histone H2AX phosphorylation: a marker for DNA damage. Methods in molecular biology. 2012; 920:613–26. [PubMed: 22941631]

45. Hoffer LJ, Levine M, Assouline S, Melnychuk D, Padayatty SJ, Rosadiuk K, et al. Phase I clinical trial of i.v. ascorbic acid in advanced malignancy. Annals of oncology: official journal of the European Society for Medical Oncology / ESMO. 2008 Nov; 19(11):1969–74. [PubMed: 18544557]

46. Moser JC, Rawal M, Wagner BA, Du J, Cullen JJ, Buettner GR. Pharmacological ascorbate and ionizing radiation (IR) increase labile iron in pancreatic cancer. Redox biology. 2013; 2:22–7. [PubMed: 24396727]

47. Olney KE, Du J, van't Erve TJ, Witmer JR, Sibenaller ZA, Wagner BA, et al. Inhibitors of hydroperoxide metabolism enhance ascorbate-induced cytotoxicity. Free radical research. 2013 Mar; 47(3):154–63. [PubMed: 23205739]

48. Batinic-Haberle I, Benov L, Fridovich I. An anionic impurity in preparations of cytochrome c interferes with assays of cationic catalysts of the dismutation of the superoxide anion radical. Analytical biochemistry. 1999 Nov 15.275(2):267. [PubMed: 10552917]

49. Batinic-Haberle I, Benov L, Spasojevic I, Fridovich I. The ortho effect makes manganese(III) meso-tetrakis(N-methylpyridinium-2-yl)porphyrin a powerful and potentially useful superoxide dismutase mimic. The Journal of biological chemistry. 1998 Sep 18; 273(38):24521–8. [PubMed: 9733746]

50. Batinic-Haberle I, Rajic Z, Benov L. A combination of two antioxidants (an SOD mimic and ascorbate) produces a pro-oxidative effect forcing Escherichia coli to adapt via induction of oxyR regulon. Anti-cancer agents in medicinal chemistry. 2011 May 1; 11(4):329–40. [PubMed: 21355843]

51. Kim MP, Evans DB, Wang H, Abbruzzese JL, Fleming JB, Gallick GE. Generation of orthotopic and heterotopic human pancreatic cancer xenografts in immunodeficient mice. Nature protocols. 2009; 4(11):1670–80.

HIGHLIGHTS

- Manganoporphyrins act synergistically with ascorbate to increase hydrogen peroxide flux
- Combination gemcitabine, MnPs, $AscH^-$ increases cytotoxicity *in vitro*
- Combination gemcitabine, MnPs, $AscH^-$ inhibits pancreatic cancer growth *in vivo*
- Double stranded DNA breaks are increased with MnP, $AscH^-$, and gemcitabine therapy
- Triple therapy does not increase systemic oxidative stress *in vivo*

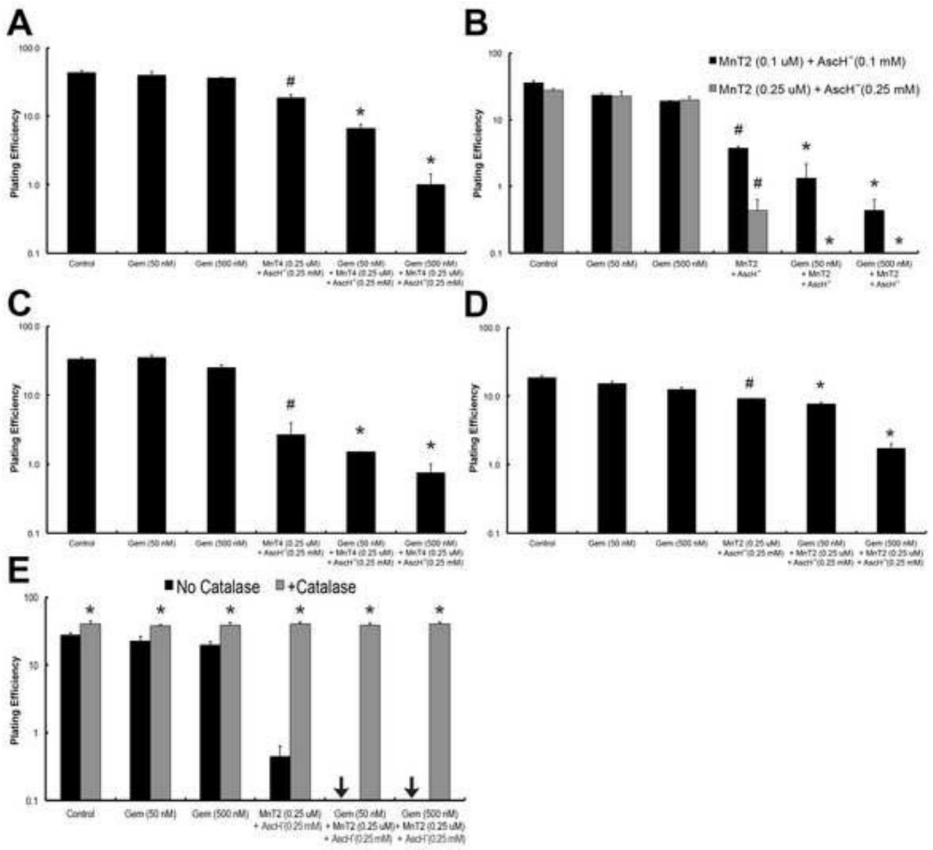

Figure 1. MnP-catalyzed ascorbate oxidation enhances gemcitabine-induced cytotoxicity

(A). Addition of MnT4MPyP (MnT4, 0.25 μM) and $AscH^-$ (0.25 mM) significantly enhances gemcitabine cytotoxicity, decreasing clonogenic survival in MIA PaCa-2 cells (*, $P < 0.01$ *vs*. the equivalent dose of gemcitabine (Gem) alone, and $P < 0.01$ *vs*. the equivalent dose of MnT4 + $AscH^-$ without Gem). MnT4MPyP (0.25 μM) and $AscH^-$ (0.25 mM) without Gem also significantly decreases clonogenic survival (#, $P < 0.01$ *vs*. Control); $n = 3$. Approximate H_2O_2 flux per cell under these conditions is 100 amol $cell^{-1}$ s^{-1} for controls and gem (50 and 500 nM), and 490 amol $cell^{-1}$ s^{-1} for Gem + MnT4 (0.25 μM) + $AscH^-$ (0.25 mM) at 0, 50 and 500 nM Gem.

(B) Addition of MnT2EPyP (MnT2, 0.1 μM) and $AscH^-$ (0.1 mM) significantly enhances Gem cytotoxicity in MIA PaCa-2 cells (*, $P < 0.01$ *vs.* the equivalent dose of Gem alone, and $P < 0.01$ *vs*. the equivalent dose of MnT2 + $AscH^-$ without Gem). MnT2EPyP (0.1 μM) and $AscH^-$ (0.1 mM) without Gem also significantly decreases clonogenic survival (#, $P < 0.01$ *vs*. Control); $n = 3$. Increasing the amount of MnT2 (0.25 μM) and $AscH^-$ (0.25 mM) completely eliminates all clonogenic survival at both 50 and 500 nM Gem (*, $P < 0.01$ *vs*. the equivalent dose of Gem alone, and $P < 0.01$ *vs*. the equivalent dose of MnT2 + $AscH^-$ without Gem). Again, MnT2EPyP (0.25 μM) and $AscH^-$ (0.25 mM) without Gem also significantly decreases clonogenic survival (#, $P < 0.01$ *vs*. Control); $n = 3$. Approximate H_2O_2 flux per cell under these conditions is 70 amol $cell^{-1}$ s^{-1} for controls and Gem (50 and 500 nM), and 450 amol $cell^{-1}$ s^{-1} for Gem + MnT2 (0.25 μM) + $AscH^-$ (0.25 mM) at 0, 50 and 500 nM Gem.

(C) The addition of MnT4 (0.25 μM) and $AscH^-$ (0.25 mM) significantly enhances Gem cytotoxicity in PANC-1 cells (*, $P < 0.01$ *vs*. the equivalent dose of Gem alone). MnT4 (0.25 μM) and $AscH^-$ (0.25 mM) without Gem also significantly reduces clonogenic survival (#, $P < 0.01$ *vs*. Control); $n = 3$. Approximate H_2O_2 flux per cell under these conditions is 150 amol $cell^{-1}$ s^{-1} for controls and Gem (50 and 500 nM), and 670 amol $cell^{-1}$ s^{-1} for Gem + MnT4 (0.25 μM) + $AscH^-$ (0.25 mM) at 0, 50 and 500 nM Gem.
(D) The addition of MnT2 (0.25 μM) and $AscH^-$ (0.25 mM) enhances Gem cytotoxicity in AsPC-1 cells (*, $P < 0.01$ *vs*. the equivalent dose of Gem alone, and $P < 0.01$ *vs*. the equivalent dose of MnT2 + $AscH^-$ without Gem). MnT2EPyP (0.25 μM) and $AscH^-$ (0.25 mM) without Gem also significantly decreases clonogenic survival (#, $P < 0.01$ *vs*. Control); $n = 3$. Approximate H_2O_2 flux per cell under these conditions is 85 amol $cell^{-1}$ s^{-1} for controls and Gem (50 and 500 nM), and 550 amol $cell^{-1}$ s^{-1} for Gem + MnT2 (0.25 μM) + $AscH^-$ (0.25 mM) at 0, 50 and 500 nM Gem.
(E) H_2O_2 mediates MnP + $AscH^-$-enhanced gemcitabine cytotoxicity. Clonogenic survival assay demonstrates that catalase completely rescued any decrease in clonogenic survival for all treatment conditions (*, $P < 0.01$); $n = 3$.

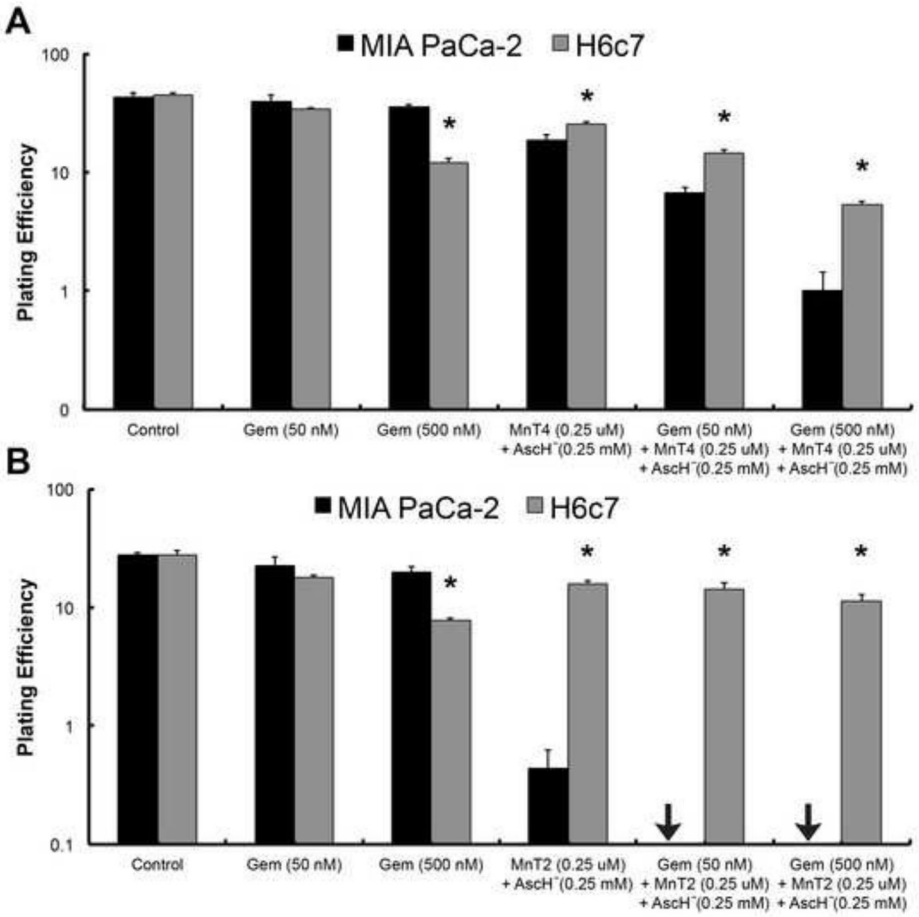

Figure 2. MnP + AscH$^-$-enhanced gemcitabine cytotoxicity selectively targets pancreatic cancer cells

(A) When cells were treated with MnT4MPyP (MnT4, 0.25 μM) + AscH$^-$ (0.25 mM), with or without gemcitabine (Gem, 50 and 500 nM), clonogenic survival was significantly reduced in MIA PaCa-2 cells *vs*. H6c7 cells (*, $P < 0.01$); $n = 3$. For MIA PaCa-2 cells, the approximate H_2O_2 flux per cell under these conditions is 99 amol cell^{-1} s^{-1} for controls and Gem (50 and 500 nM), and 489 amol cell^{-1} s^{-1} for Gem + MnT4 (0.25 μM) + AscH$^-$ (0.25 mM) at 0, 50 and 500 nM Gem. For H6c7 cells, the approximate H_2O_2 flux per cell under these conditions is 90 amol cell^{-1} s^{-1} for controls and Gem (50 and 500 nM), and 460 amol cell^{-1} s^{-1} for Gem + MnT4 (0.25 μM) + AscH$^-$ (0.25 mM) at 0, 50 and 500 nM Gem.

(B) When cells were treated with MnT2EPyP (MnT2, 0.25 μM) + AscH$^-$ (0.25 mM), with or without Gem (50 and 500 nM), clonogenic survival was again significantly reduced in MIA PaCa-2 cells *vs*. H6c7 cells (*, $P < 0.01$); $n = 3$. In both experiments, H6c7 cells were significantly more sensitive to Gem (500 nM) than MIA PaCa-2 cells (*, $P < 0.01$). For MIA PaCa-2 cells, the approximate H_2O_2 flux per cell under these conditions is 69 amol cell^{-1} s^{-1} for controls and Gem (50 and 500 nM), and 450 amol cell^{-1} s^{-1} for Gem + MnT2 (0.25 μM) + AscH$^-$ (0.25 mM) at 0, 50 and 500 nM Gem. For H6c7 cells, the approximate H_2O_2 flux per cell under these conditions is 65 amol cell^{-1} s^{-1} for controls and Gem (50 and 500 nM), and 420 amol cell^{-1} s^{-1} for Gem + MnT2 (0.25 μM) + AscH$^-$ (0.25 mM) at 0, 50 and 500 nM Gem.

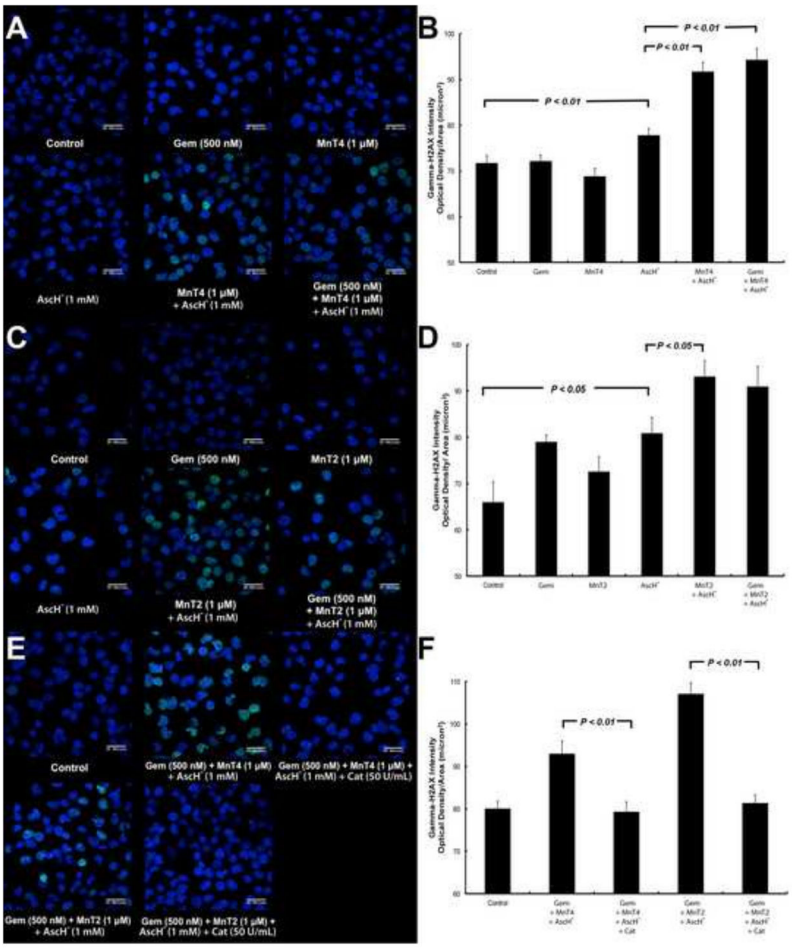

Figure 3. γH2AX immunohistochemistry reveals increased DNA damage following treatment with MnP + AscH⁻ and gemcitabine

(A) In MIA PaCa-2 cells, MnT4 + AscH⁻ and MnT4 + AscH⁻ + Gem demonstrated increased γH2AX fluorescence. Blue fluorescence = DAPI nuclear staining. Green fluorescence = γH2AX protein.

(B) Quantification of fluorescence per area in images in Figure 3A. MnT4 + AscH⁻ and MnT4 + AscH⁻ + Gem showed significant increases in γH2AX fluorescence compared to control, Gem, MnT4, and AscH⁻ treated cells ($P < 0.01$). No difference between MnT4 + AscH⁻ and MnT4 + AscH⁻ + Gem was observed.

(C) There is an increase in γH2AX fluorescence in MIA PaCa-2 cells treated with MnT2 + AscH⁻ and MnT2 + AscH⁻ + Gem.

(D) Quantification of fluorescence per area in images in Figure 3C. An increase in γH2AX fluorescence was observed in cells treated with MnT2 + AscH⁻ and MnT2 + AscH⁻ + Gem *vs*. control, Gem and MnT2-treated cells ($P < 0.05$). There was no difference observed as the result of the addition of MnT2 + AscH⁻ to Gem.

(E) γ-H2AX immunohistochemistry on MIA PaCa-2 cells demonstrates increased γH2AX fluorescence following combination treatments, which was reversed by catalase pretreatment.

(F) Quantification of fluorescence per area in images in Figure 3E. When treated with catalase, γH2AX fluorescence observed in MnT4 + $AscH^-$ + Gem and MnT2 + $AscH^-$ + Gem-treated cells is absent ($P < 0.01$).

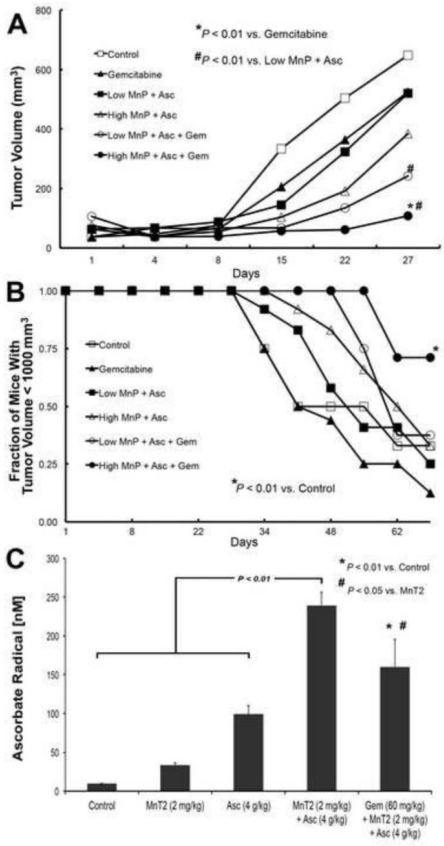

Figure 4. MnP + AscH$^-$ enhances gemcitabine-induced cytotoxicity *in vivo*

(A) Linear mixed effects regression models were used to estimate and compare group specific tumor growth curves from MIA PaCa-2 tumor xenografts in 30 day old athymic nude mice. Tumor growth was significantly inhibited in mice treated with high dose MnP + AscH$^-$ + Gem vs. control mice, mice treated with Gem alone (*, $P < 0.01$) and mice treated with the combination of "Low MnP + AscH$^-$" (#, $P < 0.01$). Furthermore, tumor growth was significantly inhibited in mice treated with low dose MnP + AscH$^-$ + Gem vs. control mice and mice treated with the combination of "Low MnP + AscH$^-$" (#, $P < 0.01$). Controls, $n = 12$; Gemcitabine, $n = 8$; Low MnP + AscH$^-$, $n = 8$; High MnP + AscH$^-$, $n = 8$; Low MnP + AscH$^-$ + Gem, $n = 8$; High MnP + AscH$^-$ + Gem, $n = 8$.

(B) Kaplan-Meier style plots demonstrating the fraction of mice remaining in each treatment group with tumors smaller than 1000 mm^3 as function of time. The log-rank test was used for pairwise treatment group comparisons and demonstrated a significant increase in the fraction of mice with tumors smaller than 1000 mm^3 at day 69 in the group receiving high dose MnP + AscH$^-$ + Gem vs. control mice (*, $P < 0.01$).

(C) In separate groups of athymic nude mice that were treated for 5 days, whole blood was collected after a fatal dose of ketamine, 1 hour after the final intraperitoneal dose, and was used to obtain EPR spectra. In control mice, [Asc$^{\bullet -}$] is below the limit of detection (< 10 nM). [Asc$^{\bullet -}$]$_{ss}$ increases to 34 nmol/L upon treatment with MnT2 (0.2 mg/kg i.p.). After injection of pharmacologic AscH$^-$ (4 g/kg i.p.), [Asc$^{\bullet -}$]$_{ss}$ increased to 99 nmol/L. Combining both MnT2 and AscH$^-$ increased [Asc$^{\bullet -}$]$_{ss}$ to 239 nmol/L. ($P < 0.01$ *vs.* control,

$AscH^-$, and MnT2). When MnT2 and $AscH^-$ were combined with gemcitabine, $[Asc^{\bullet -}]_{ss}$ was 160 nmol/L ($P < 0.01$ *vs*. control, $P < 0.05$ *vs*. MnT2); $n = 3$ mice for each determination.

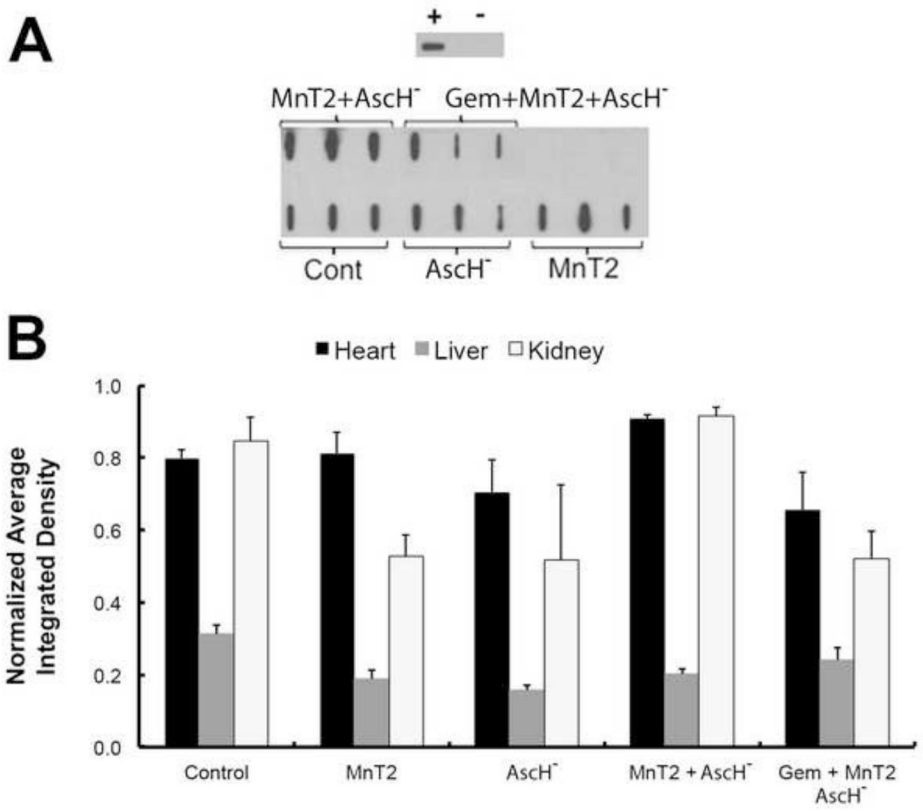

Figure 5. MnP + AscH$^-$ and gemcitabine does not alter systemic levels of 4HNE-modified proteins *in vivo*

(A) Representative 4HNE dot blot. Purified bovine serum albumin (BSA) was reacted with excess purified 4-HNE to create a positively labeled protein control seen in the upper panel. Negative control is unreacted purified BSA. Blot for 4-HNE modified proteins in cardiac muscle showed no changes in immunoreactive protein after any of the treatments when compared to controls.

(B) Quantification of dot blots for 4-HNE modified proteins in mouse heart, liver and kidney homogenates demonstrated no difference in immuno-reactive protein after any of the treatments when compared to controls; $n = 3$.

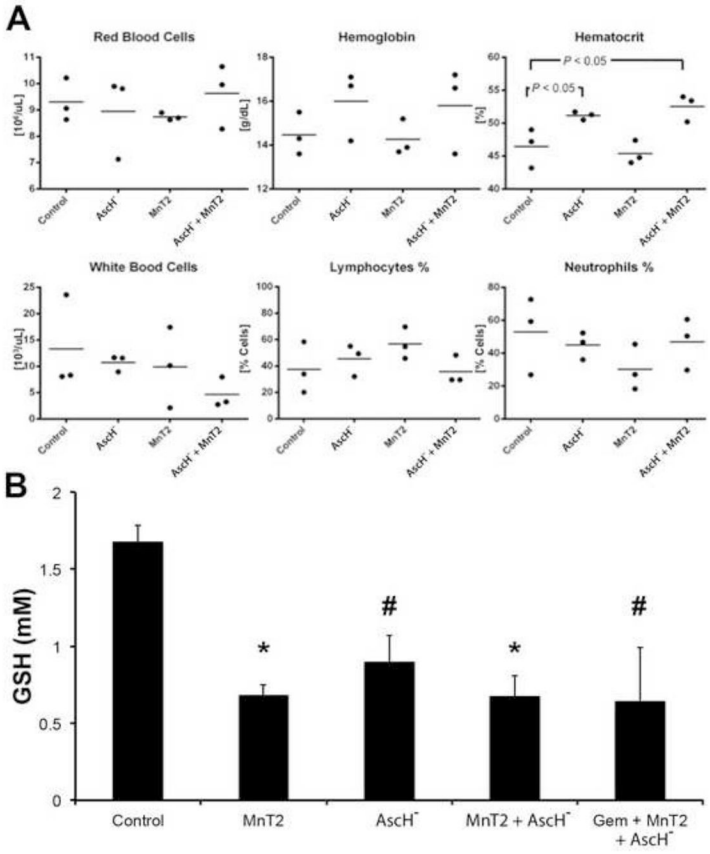

Figure 6. Effects of combination MnP + AscH$^-$ and gemcitabine on circulating hematologic cells

(A) Complete blood counts and differential in control mice and those treated with AscH$^-$, MnT2, and AscH$^-$ + MnT2. Hematocrit (Hct) was increased in mice treated with ascorbate ($P < 0.05$ *vs*. controls), there were no significant changes in all other measures compared to controls; $n = 3$.

(B) Total erythrocyte glutathione (tGSH) constitutes the largest redox buffer pool. Blood was collected from separate groups of mice after treatments and assayed for the intracellular concentration of GSH in RBCs. All treatments resulted in decreased tGSH *vs*. controls ($P < 0.01$ for MnT2 and AscH$^-$ + MnT2; $P < 0.05$ for AscH$^-$ and gem + MnT2 + AscH$^-$); $n = 3$.